



The impact of
volcanic aerosol on
the NH stratospheric
polar vortex

M. Toohey et al.

The impact of volcanic aerosol on the Northern Hemisphere stratospheric polar vortex: mechanisms and sensitivity to forcing structure

M. Toohey¹, K. Krüger^{1,2}, M. Bittner^{3,4}, C. Timmreck³, and H. Schmidt³

¹GEOMAR Helmholtz Centre for Ocean Research Kiel, Kiel, Germany

²University of Oslo, Department of Geosciences, Oslo, Norway

³Max Planck Institute for Meteorology, Hamburg, Germany

⁴International Max Planck Research School on Earth System Modeling (IMPRS), Hamburg, Germany

Received: 9 May 2014 – Accepted: 10 June 2014 – Published: 25 June 2014

Correspondence to: M. Toohey (mtoohey@geomar.de)

Published by Copernicus Publications on behalf of the European Geosciences Union.

Title Page

Abstract

Introduction

Conclusions

References

Tables

Figures



Back

Close

Full Screen / Esc

Printer-friendly Version

Interactive Discussion



Abstract

Observations and simple theoretical arguments suggest that the Northern Hemisphere (NH) stratospheric polar vortex is stronger in winters following major volcanic eruptions. However, recent studies show that climate models forced by prescribed volcanic aerosol fields fail to reproduce this effect. We investigate the impact of volcanic aerosol forcing on stratospheric dynamics, including the strength of the NH polar vortex, in ensemble simulations with the Max Planck Institute Earth System Model. The model is forced by four different prescribed forcing sets representing the radiative properties of stratospheric aerosol following the 1991 eruption of Mt. Pinatubo: two forcing sets are based on observations, and are commonly used in climate model simulations, and two forcing sets are constructed based on coupled aerosol–climate model simulations. For all forcings, we find that temperature and zonal wind anomalies in the NH high latitudes are not directly impacted by anomalous volcanic aerosol heating. Instead, high latitude effects result from robust enhancements in stratospheric residual circulation, which in turn result, at least in part, from enhanced stratospheric wave activity. High latitude effects are therefore much less robust than would be expected if they were the direct result of aerosol heating. While there is significant ensemble variability in the high latitude response to each aerosol forcing set, the mean response is sensitive to the forcing set used. Significant differences, for example, are found in the NH polar stratosphere temperature and zonal wind response to two different forcing data sets constructed from different versions of SAGE II aerosol observations. Significant strengthening of the polar vortex, in rough agreement with the expected response, is achieved only using aerosol forcing extracted from prior coupled aerosol–climate model simulations. Differences in the dynamical response to the different forcing sets used imply that reproducing the polar vortex responses to past eruptions, or predicting the response to future eruptions, depends on accurate representation of the space-time structure of the volcanic aerosol forcing.

The impact of volcanic aerosol on the NH stratospheric polar vortex

M. Toohey et al.

Title Page

Abstract

Introduction

Conclusions

References

Tables

Figures



Back

Close

Full Screen / Esc

Printer-friendly Version

Interactive Discussion



1 Introduction

The Northern Hemisphere (NH) stratospheric winter polar vortex, which shows considerable interannual and intra-seasonal variability, has been observed to be stronger than normal in winters after major volcanic eruptions (Kodera, 1995; Labitzke and van Loon, 1989). While this observation is based on a relatively small sample (limited to the winters after the 1963 Agung, 1982 El Chichón and 1991 Pinatubo eruptions), the theoretical argument to explain such a strengthening appears clear: namely, that heating of the lower stratosphere through the absorption of radiation by volcanic sulfate aerosols enhances the equator-to-pole temperature gradient in the lower stratosphere, which, through the thermal wind equation, leads to stronger westerly winds (Robock, 2000 and references therein). Satellite observations clearly show a warming of the tropical lower stratosphere after volcanic eruptions (Labitzke and McCormick, 1992), so changes in meridional temperature gradients and zonal winds are logical consequences. The degree to which secondary feedback mechanisms – such as changes in ozone or upward propagating planetary waves (e.g., Graf et al., 2007; Stenchikov et al., 2006) – also affect the vortex strength is at present unclear.

Post-volcanic strengthening of the NH polar vortex is an important step in a proposed mechanism which explains observed changes in surface climate in post-eruption winters (Kodera, 1994; Perlwitz and Graf, 1995). Specifically, it is thought that through stratosphere–troposphere coupling (Baldwin and Dunkerton, 2001; Gerber et al., 2012) the volcanically-induced strong stratospheric polar vortex leads to the observed positive anomalies in surface dynamical indexes such as the Northern Annular Mode (NAM) or North Atlantic Oscillation (NAO) (Christiansen, 2008). Such dynamical changes lead to the “winter warming” pattern of post-volcanic temperature anomalies (Robock and Mao, 1992), which is characterized by warmer temperatures over large regions of the NH continents during winter which oppose the overall cooling impact of the volcanic aerosols on the surface. On the other hand, in a model study, Stenchikov (2002) found that a positive phase of the NAM was also produced in an experiment in which only the

The impact of volcanic aerosol on the NH stratospheric polar vortex

M. Toohey et al.

Title Page

Abstract

Introduction

Conclusions

References

Tables

Figures



Back

Close

Full Screen / Esc

Printer-friendly Version

Interactive Discussion



The impact of volcanic aerosol on the NH stratospheric polar vortex

M. Toohey et al.

Title Page

Abstract

Introduction

Conclusions

References

Tables

Figures



Back

Close

Full Screen / Esc

Printer-friendly Version

Interactive Discussion



5 tropospheric impact of volcanic aerosols was included, implying that aerosol heating in the lower tropical stratosphere is not necessary to force a positive NAM response. Whatever the mechanisms, observations show that 11 out of 13 eruptions since 1870 were followed by positive wintertime NAO values (Christiansen, 2008): the apparent robustness of this post-eruption dynamical response should allow for enhanced skill in seasonal prediction for winters which follow volcanic eruptions (e.g., Marshall et al., 2009).

10 While a number of early model simulations reported qualified success in simulating the atmospheric dynamical response to volcanic eruptions (e.g., Graf et al., 1993; Kirchner et al., 1999; Rozanov, 2002; Shindell et al., 2001), assessments of the multi-model ensembles of the Coupled Model Intercomparison Projects (CMIP) 3 and 5 showed no significant winter warming response to prescribed volcanic forcing, nor did they show significant anomalies in post-eruption dynamical quantities in the stratosphere or at the surface (Driscoll et al., 2012; Stenchikov et al., 2006). It has been suggested that in order for a model to successfully respond to volcanic forcing, it should include a reasonably well-resolved stratosphere (Shindell, 2004; Stenchikov et al., 2006). However, analysis of the CMIP5 ensemble revealed no appreciable systematic difference in post-eruption geopotential height anomalies to volcanic aerosol forcing between models with or without well-resolved stratospheres (Charlton-Perez et al., 2013).

20 Most model simulations which incorporate the impact of volcanic eruptions, such as the CMIP3 and 5 historical simulations, do so using prescribed volcanic aerosol fields, which have associated uncertainties. In this study we investigate how the response of the atmosphere to volcanic aerosol forcing depends on the prescribed aerosol forcing used in the simulation. We use one CMIP5 model, the MPI-ESM, and focus on the first winter after Mt. Pinatubo, the period of strongest volcanic forcing within the era of satellite observations. We run ensemble simulations using four different forcing data sets: two observation-based forcing sets, based primarily on different versions of SAGE II aerosol extinction measurements, and two model-constructed aerosol forcing sets.

The impact of volcanic aerosol on the NH stratospheric polar vortex

M. Toohey et al.

[Title Page](#)[Abstract](#)[Introduction](#)[Conclusions](#)[References](#)[Tables](#)[Figures](#)[Back](#)[Close](#)[Full Screen / Esc](#)[Printer-friendly Version](#)[Interactive Discussion](#)

By assessing the model response to these forcing sets, we investigate (1) the mechanisms linking volcanic aerosol heating in the lower tropical stratosphere and NH winter vortex strength, (2) what stratospheric circulation responses to volcanic aerosol forcing are robustly produced by the model and forcings, and (3) the sensitivity of the vortex response to changes in the space-time structure of the volcanic forcing.

2 Data and methods

2.1 ERA-Interim

To illustrate the observed atmospheric response to volcanic eruptions, ERA-Interim reanalysis (Dee et al., 2011) temperature and zonal wind fields are examined after the eruptions of El Chichón (1982) and Pinatubo (1991). Post-eruption winter anomalies are constructed for the two winters after each eruption by differencing post-eruptive December-to-February (DJF) mean fields with fields averaged for 3 (El Chichón) and 5 (Pinatubo) years before the eruption (the shorter reference period for El Chichón resulting from the fact that the ERA-Interim data set begins in 1979). Differences in post-eruption anomalies for Pinatubo are not strongly dependent on the choice of a 3, 4 or 5 year reference period.

2.2 MPI-ESM

The MPI-ESM is a full Earth System model, with atmosphere, ocean, carbon cycle, and vegetation components. Major characteristics of the full ESM and its performance in the CMIP5 experiments are described by Giorgetta et al. (2013). The “low resolution” model configuration (MPI-ESM-LR) is used here, with horizontal resolution of the atmospheric component given by a triangular truncation at 63 wave numbers (T63) and 47 vertical layers extending to 0.01 hPa. Unlike higher resolution configurations, the LR version has no internally generated Quasi Biennial Oscillation (QBO).

The impact of volcanic aerosol on the NH stratospheric polar vortex

M. Toohey et al.

Title Page

Abstract

Introduction

Conclusions

References

Tables

Figures



Back

Close

Full Screen / Esc

Printer-friendly Version

Interactive Discussion



anomalies between 60 and 80° N in Fig. 2. However, the ensemble variability of the simulations is pronounced, with 3 members showing a weakened polar vortex with positive temperature anomalies over the polar cap and negative wind anomalies between 60 and 80° N. From the full 12-member ensemble, two subsets were defined based on the zonal wind anomalies, with strong and weak vortex composites (hereafter SVC and WVC) selected respectively as the 3 members with the most positive and most negative zonal wind anomalies at 50 hPa and 70° N. Aerosol properties (aerosol extinction at 0.55 μm and effective radius) for these two composites were collected for use in MPI-ESM simulations. SVC and WVC zonal mean AOD timeseries, scaled to 1 μm so as to be consistent with the observation-based AOD timeseries, are shown in Fig. 1.

2.5 Experiments

The forcing sets described above were used to force four twelve-member ensemble simulations of the Pinatubo eruption time period. The number of MPI-ESM realizations used here is therefore notably greater than the three MPI-ESM realizations used in prior single- (Schmidt et al., 2013) or multi-model (Charlton-Perez et al., 2013; Driscoll et al., 2012) investigations of the CMIP5 historical simulations. Six of the twelve unique initial condition states (at June 1991) were taken from six independent, pre-existing CMIP5 historical simulations. In order to increase the ensemble size from 6 to 12, the 6 historical simulations were restarted in 1980 with a small atmospheric perturbation applied, and integrated until 1991. All simulations were therefore forced with S98 volcanic forcing up until June 1991, at which point forcing either continued as S98, or switched to one of the other forcings.

A control ensemble (CTL) is based on the five year period 1986–1990 for the original six historical simulations used to produce the initial conditions, comprising in total 30 years, during which the other external forcings are negligibly different from 1991–1992 conditions. Anomalies for the volcanic ensembles are computed by differencing ensemble mean results with the CTL ensemble mean.

The impact of volcanic aerosol on the NH stratospheric polar vortex

M. Toohey et al.

Title Page

Abstract

Introduction

Conclusions

References

Tables

Figures



Back

Close

Full Screen / Esc

Printer-friendly Version

Interactive Discussion

NH winter polar vortex, by $\sim 6 \text{ m s}^{-1}$. Such a simple average with a small sample size does not completely remove the influences of variability resulting from other forcing terms – notably the solar activity was at a minimum at the times of both the El Chichón and Pinatubo eruptions, and El Niño events were observed in the first winters after both eruptions – but the composite temperature and zonal wind anomaly structure is certainly a better approximation of the direct volcanic impact than anomalies in any single post-volcanic year. For comparison, single winter anomalies are shown for the first winter after the Pinatubo eruption. Temperature anomalies for DJF 1991/92 roughly follow the structure of the volcanic composite, albeit with tropical positive anomalies located at higher altitudes, and weaker polar lower stratosphere cooling. Post-Pinatubo zonal wind anomalies in the tropics reflect the state of the QBO at the time, with negative (easterly) wind anomalies in the middle stratosphere ($\sim 50\text{--}15 \text{ hPa}$) and positive (westerly) anomalies in the upper stratosphere ($15\text{--}2 \text{ hPa}$). The polar vortex in the first post-Pinatubo winter was actually not as clearly enhanced as the 4 year composite, with positive zonal wind anomalies only in the mid to lower polar stratosphere centered at $\sim 70^\circ \text{ N}$. It is likely that in addition to the volcanic forcing, the vortex in DJF 1991/92 shows weakened conditions due to the concurrent forcing of the El Niño and QBO easterly phase. Based on these arguments, it can be hypothesized that the pure response of stratosphere to Pinatubo aerosol forcing would have the approximate structure of the composite response shown in Fig. 3 (left), albeit with greater amplitude, since the aerosol optical depth and hence aerosol radiative heating during the first post-Pinatubo winter is the strongest of the years used in the volcanic composite. This “expected” response in the first post-Pinatubo winter is based on a small sample size of observations, and an assumption of linear response to the magnitude of volcanic forcing, however, in light of limited evidence, it represents a best first-order, observation-based expectation, consistent with that assumed explicitly or implicitly in prior studies.

S98 leading to slightly larger Q^{aer} values in the NH polar lower stratosphere than for SAGE_4 λ .

3.2.2 Temperature and zonal wind response

5 First post-eruption NH winter temperature and zonal wind anomalies for the S98 and SAGE_4 λ ensembles are shown in Fig. 5. Positive temperature anomalies in the tropical lower stratosphere are found in both ensembles. Both ensembles also show negative temperature anomalies in the troposphere, extending to the surface between approximately 60° S–60° N. In agreement with Q^{aer} of Fig. 4, SAGE_4 λ tropical temperature anomalies are greater in magnitude, with peak values of 4.8 K compared to 3.6 K
10 for S98. Temperature anomalies are also shifted in height between the two ensembles, with peak temperature anomalies located at 30 hPa for SAGE_4 λ , compared to 50 hPa for S98. Differences in tropical temperature anomalies between the two ensembles (right-most column of Fig. 5) are significant at the 95 % confidence level between approximately 200 and 20 hPa.

15 In the NH high latitude stratosphere, temperature anomalies are clearly different between the two ensembles. The temperature anomaly structure in the S98 ensemble is consistent with that shown by Schmidt et al. (2013) for three MPI-ESM realizations (also using S98 forcing), with (insignificant) negative temperature anomalies in the lower stratosphere and positive anomalies in the upper stratosphere and mesosphere.
20 Conversely, the SAGE_4 λ forcing leads to positive temperature anomalies throughout the whole high latitude stratosphere. The magnitude of the difference in temperatures for the two ensembles is significant at the 95 % level throughout much of the polar stratosphere.

25 Zonal wind anomalies, also shown in Fig. 5, are positive in the SH in both ensembles, representing a weakening of the summer easterlies by 4–6 m s⁻¹. Also, negative wind anomalies are found at 30° N, 100 hPa, in both ensembles, which represents a weakening of the upper, northward flank of the NH subtropical tropospheric jet by 2–4 m s⁻¹. In the NH high latitudes, the wind anomalies are consistent with the temperature

The impact of volcanic aerosol on the NH stratospheric polar vortex

M. Toohey et al.

Title Page

Abstract

Introduction

Conclusions

References

Tables

Figures



Back

Close

Full Screen / Esc

Printer-friendly Version

Interactive Discussion



(around 30° N, 10 hPa, Fig. 6f and g) is found in both ensembles. Wave drag in this location is especially important for forcing the residual circulation (Shepherd and McLandress, 2011), and the poleward NH residual circulation stream function is found to be enhanced in both ensembles (Fig. 6j and k).

While enhanced residual circulation is found for both ensembles, the strength of the enhancement and the meridional extension is notably (but not significantly) different. The residual circulation anomalies are stronger, and extend farther polewards in the SAGE_4λ ensemble. This may be related to the fact that midlatitude-middle stratosphere EPFD negative anomalies are slightly stronger for SAGE_4λ than S98 (Fig. 6h), and it may be that the differences in EPFD in the upper stratosphere (60° N, 1 hPa) also play some role in driving the different residual circulation magnitudes. In the NH high latitudes, the S98 ensemble shows insignificant positive anomalies in EPFD, i.e., less than normal wave drag, while the anomalies for SAGE_4λ are less notable. For S98, such EPFD anomalies are consistent with an equatorward anomaly in residual circulation at the high latitudes.

The volcanically-induced residual circulation anomalies drive adiabatic heating anomalies where vertical motions are induced. Temperature tendency anomalies due to residual vertical velocity (hereafter $dT_{\overline{w}}$, Fig. 6n and o) show clearly the tropical cooling associated with anomalous vertical upwelling, and heating at the mid and high latitudes due to anomalous downwelling. The structures of the $dT_{\overline{w}}$ fields at high latitudes are clearly consistent with the temperature anomalies of Fig. 5, and explain the difference in high latitude heating between S98 and SAGE_4λ as differences in the form of the downwelling-induced heating. The stronger and larger residual circulation cell in SAGE_4λ leads to heating of the lower stratosphere extending from 30–90° N, which is strongest at polar latitudes. In contrast, the weaker and narrower meridional circulation cell in S98 leads to lower stratospheric heating in the midlatitudes, and in fact relative upwelling at polar latitudes leads to cooling there.

Lower stratospheric temperature and heating anomalies are examined in more detail in Fig. 7. Ensemble mean temperature anomalies, averaged vertically over 100–20 hPa

The impact of volcanic aerosol on the NH stratospheric polar vortex

M. Toohey et al.

Title Page

Abstract

Introduction

Conclusions

References

Tables

Figures



Back

Close

Full Screen / Esc

Printer-friendly Version

Interactive Discussion



the original simulations. This experiment therefore tests to what degree the vortex response can be controlled through changes in the prescribed aerosol forcing fields.

3.3.1 Aerosol extinction and radiative heating

Figure 8 shows DJF 1 μm aerosol extinction (EXT) for the SVC and WVC forcing sets. Compared to the observation-based forcing sets, both model-based forcing sets have greater magnitudes of aerosol extinction, especially in the high latitudes. The model-based extinctions also have stronger gradients (both vertical and horizontal) across the tropopause. The primary difference between the SVC and WVC forcings is the hemispheric partitioning of the aerosol extinction, with WVC having larger extinctions in the NH than SVC. We interpret this difference as a result of wave driven circulation in the NH: in cases of strong NH wave forcing in the original MAECHAM5-HAM runs, a stronger residual circulation transports more aerosol from the tropical region towards the NH, while also disturbing the NH polar vortex. Therefore, by selecting cases of weak polar vortex, we also select cases of strong northward aerosol transport. Another major difference is the magnitude of extinction in the NH high latitudes, and therefore the gradient in extinction around 60° N. The stronger aerosol extinction gradient in the SVC forcing set is obviously a result of the strong vortex in the MAECHAM5-HAM simulations, which inhibits mixing of aerosol into the polar cap. In the tropics, SVC and WVC have very small differences, and their vertical distribution is almost identical.

Q^{aer} values, also shown in Fig. 8, are more similar to the observation-based Q^{aer} values than the extinctions: the differences in high latitude extinction have relatively little impact on the Q^{aer} differences due to the much weaker LW radiation field here than in the tropics. Differences in Q^{aer} between the two model-based forcing ensembles are relatively small (compared to differences between the two observation-based forcing ensembles), and are characterized primarily by the north–south shift between the two forcing sets, and the gradients in Q^{aer} at 60° S and 60° N. At high latitudes, Q^{aer} values are apparently not strongly dependent on the aerosol extinction, e.g., SVC has smaller aerosol extinction values in polar latitudes than WVC, but shows larger Q^{aer} .

The impact of volcanic aerosol on the NH stratospheric polar vortex

M. Toohey et al.

Title Page

Abstract

Introduction

Conclusions

References

Tables

Figures



Back

Close

Full Screen / Esc

Printer-friendly Version

Interactive Discussion



This is likely due to the fact that the net (absorption-emission) long wave heating rate is strongly temperature dependent because of the temperature dependence of the emission. As shown below, the SVC ensemble is characterized by a colder polar vortex than for WVC, which should lead to less emission and thus larger net heating.

3.3.2 Temperature and zonal wind response

First post-eruption NH winter temperature and zonal wind anomalies for the SVC and WVC ensembles are shown in Fig. 9. Temperature anomalies in the tropics and mid-latitudes are quite similar in structure between the two ensembles and similar to the observation-based forced ensembles, with negative anomalies in the troposphere, positive anomalies in the lower stratosphere, and negative anomalies again in the upper stratosphere. In the NH high latitudes, however, the temperature responses are quite different in structure between the SVC and WVC ensembles. The SVC ensemble produces a NH high latitude temperature anomaly pattern similar to the S98 ensemble with significant warming in the upper stratosphere. WVC, on the other hand, gives a temperature anomaly pattern similar to the SAGE_4 λ ensemble, with insignificant positive temperature anomalies in the polar lower and middle stratosphere. Differences between the two forcing sets are significant only in the high latitude upper stratosphere.

Zonal wind anomalies for the model-based forcing ensembles follow from the temperature anomalies. Like the observation-based ensembles, significant zonal wind anomalies include a weakening of the easterly summer circulation in the SH, and a weakening of the upper, northward flank of the subtropical jets of both hemispheres. The SVC ensemble produces a significant strengthening of the NH polar vortex, with peak zonal wind anomalies approaching 10 m s^{-1} . The WVC ensemble produces no significant change in NH vortex winds. While the SVC polar zonal wind anomalies are significant, given the variability of the two forced ensembles, the difference (SVC-WVC) shows significance only at scattered locations in the polar latitudes.

The impact of volcanic aerosol on the NH stratospheric polar vortex

M. Toohey et al.

Title Page

Abstract

Introduction

Conclusions

References

Tables

Figures



Back

Close

Full Screen / Esc

Printer-friendly Version

Interactive Discussion



3.3.3 Wave activity and residual circulation

As in the observation-based ensembles, both model-based forced ensembles show positive F_z anomalies throughout the SH stratosphere and negative anomalies in the subtropical tropopause region (Fig. 10b and c). Positive F_z anomalies are found at the high latitude lower stratosphere, extending upwards and slanting equatorward with height. However, these positive F_z anomalies are significant only for WVC in the lower stratosphere around 60° N. Differences in F_z between the two ensembles (Fig. 10d) are generally not significant.

Like the observation-based ensembles, negative EP-flux divergence (wave drag) is significantly enhanced in the SH stratosphere and marginally in the NH midlatitude middle stratosphere (Fig. 10f and g). Residual circulation anomalies (Fig. 10j and k) show significant counter-clockwise circulation in the SH, and insignificant clockwise circulation cells in the NH, which are confined to 0–45° N in the SVC ensemble, and extending 0–90° N in the WVC ensemble. Temperature tendency anomalies due to residual vertical velocity ($dT_{\vec{w}}$, Fig. 10n and o) show clearly the tropical cooling associated with vertical upwelling, and heating at the mid and high latitudes due to downwelling. The broad residual circulation anomaly cell in the WVC ensemble leads to dynamical heating of the polar lower stratosphere, while the narrower poleward cell in SVC leads to significant heating in the midlatitude lower stratosphere.

Lower stratospheric temperature and heating anomalies for the SVC and WVC ensembles are examined in more detail in Fig. 11. Ensemble mean temperature anomalies, averaged vertically over 100–20 hPa show again the negative and positive temperature anomalies over polar latitudes for the SVC and WVC ensembles, respectively. As was the case for the observation-based forced ensembles, the differences in polar latitude temperature anomalies result from differences in dynamical heating in the high latitudes rather than differences in Q^{aer} (Fig. 11c). Likewise, differences in the meridional gradients in temperature anomalies (Fig. 11b) are the result of differences in dynamical heating due to vertical advection (Fig. 11d). These results are similar to

The impact of volcanic aerosol on the NH stratospheric polar vortex

M. Toohey et al.

[Title Page](#)[Abstract](#)[Introduction](#)[Conclusions](#)[References](#)[Tables](#)[Figures](#)[Back](#)[Close](#)[Full Screen / Esc](#)[Printer-friendly Version](#)[Interactive Discussion](#)

the results of the observation-based ensembles, and underscore the point that temperature gradients at the high latitudes are controlled by the structure of the volcanically induced residual circulation anomalies rather than the direct aerosol heating.

3.4 MPI-ESM results: integrated results

5 Despite some differences in the MPI-ESM responses to the different forcing fields, a number of responses are robust across all forcing sets used. To illustrate this, the four volcanic ensembles are concatenated into one “super” ensemble (ALL), and ensemble mean anomalies of a number of dynamical fields are shown in Fig. 12. DJF temperature anomalies for the ALL ensemble are significant throughout most of the tropopause and lower-to-middle stratosphere, except, importantly, in the NH polar region. Significant zonal wind responses in the ALL ensemble include weakening of the subtropical jets at $\sim 30^\circ$ and ~ 100 hPa of both hemispheres, and a weakening of the SH stratospheric summertime easterlies. No significant zonal wind anomalies are found in the NH stratosphere. Significant F_z anomalies include negative anomalies in the midlatitude tropopause regions of both hemispheres, but an increase in the high latitude F_z (from ~ 50 – 90° of both hemispheres). Significant positive F_z anomalies are also found in the mid to high-latitude (45 – 65° N) lower stratosphere (100–30 hPa), in the subtropical upper stratosphere, and throughout much of the SH stratosphere. Negative EP-flux divergence (i.e., enhanced wave drag) is similarly found in the subtropical upper stratosphere ($\sim 30^\circ$ N, ~ 70 – 2 hPa), and throughout much of the SH stratosphere. Such wave drag forces significant residual circulation anomalies in both hemispheres, and resulting cooling of the tropical stratosphere, and heating of the mid to high latitude stratosphere of each hemisphere. Significant heating via vertical advection is however constrained to 30 – 60° N, since, as shown before, $\overline{w^*}$ anomalies and connected heating rates are highly variable in the NH winter vortex region.

25 The anomalous dynamical situation sketched above leads to atypical relationships between dynamical quantities in post-volcanic winters. For example, Fig. 13 (upper left) shows the relationship between polar vortex wind (u at 10 hPa, 60° N, hereafter u_{vortex})

The impact of volcanic aerosol on the NH stratospheric polar vortex

M. Toohey et al.

Title Page

Abstract

Introduction

Conclusions

References

Tables

Figures



Back

Close

Full Screen / Esc

Printer-friendly Version

Interactive Discussion



The impact of volcanic aerosol on the NH stratospheric polar vortex

M. Toohey et al.

Title Page

Abstract

Introduction

Conclusions

References

Tables

Figures



Back

Close

Full Screen / Esc

Printer-friendly Version

Interactive Discussion



and lower stratosphere polar temperature (T at 50 hPa, 60–90° N average, hereafter T_{vortex}). The linear relationship apparent in the control run is shifted in the volcanic simulations: for a given lower stratospheric polar T_{vortex} , the associated u_{vortex} is typically $\sim 5 \text{ m s}^{-1}$ stronger in the volcanic runs than in CTL. This relationship is explored further by plotting both u_{vortex} and T_{vortex} vs. F_z at 100 hPa averaged over 45–75° N (hereafter $F_{z,100}$, a common scalar metric for wave activity entering the extratropical stratosphere (Newman et al., 2001; Polvani and Waugh, 2004)). While the relationship between T_{vortex} and $F_{z,100}$ is roughly consistent in the volcanic and CTL ensembles, u_{vortex} is seen to be stronger for any particular $F_{z,100}$ value in the volcanic runs compared to the CTL ensemble. This upward shift of about 5 m s^{-1} may be considered the “pure” zonal wind response to the anomalous temperatures of the lower stratosphere, independent of changes in wave activity. However, the volcanic ensembles show positive anomalies in $F_{z,100}$, so in addition to the thermal impact, the zonal wind of the volcanic ensembles is reduced due to the increased wave activity and hence wave drag. Post-volcanic anomalies in $F_{z,100}$ thus exert a negative feedback on the wind anomalies driven by changes in the lower stratosphere temperature gradient.

Finally, in Fig. 14, we examine changes in tropical upwelling in the simulation ensembles, which is a typical metric for the strength of the wave-driven stratospheric residual circulation, or Brewer–Dobson circulation (BDC). Tropical upwelling is computed as the area averaged \overline{w}^* over the latitudes for which it is positive at a certain pressure level, i.e., between the “turnaround latitudes”. Compared to the CTL ensemble, the volcanic ensembles actually show a decrease in tropical upwelling at 70 hPa, which is the standard height level often used to quantify the strength of the BDC (e.g., Seviour et al., 2012). However, upwelling is stronger at higher levels, for example at 30 hPa, as shown in Fig. 14 (right). This can also be seen in the residual circulation anomalies of Fig. 12: the cell of positive residual circulation in the ALL ensemble begins only at approximately 50 hPa. Below this level, there is actual a weakening of the residual circulation cell.

4 Discussion

A major result of the preceding sections is that the temperature structure of the lower stratosphere in post-volcanic winters in the high latitudes is controlled primarily by induced residual circulation anomalies. Post volcanic-eruption enhancement of the stratospheric residual circulation (or BDC) have been suggested based on previous model studies (Pitari and Mancini, 2002; Pitari, 1993). Graf et al. (2007) assessed the observational record and found evidence of increased winter stratospheric wave activity after three eruptions (Agung El Chichón and Pinatubo). Poberaj et al. (2011) showed that anomalously strong EP-fluxes occurred in the SH after Pinatubo. Such increases in winter stratospheric wave activity are likely a result of changes in the wave propagation conditions of the stratosphere following aerosol radiative heating, allowing more planetary waves to propagate upwards. Similar arguments explain climate models' predicted increase in future stratospheric residual circulation due to changes in the atmospheric temperature structure due to climate change (Garcia and Randel, 2008; McLandress and Shepherd, 2009; Shepherd and McLandress, 2011), which also enhances the meridional temperature gradient in the lower stratosphere, albeit at lower altitudes.

The residual circulation anomalies induced by the volcanic forcing in the ensembles strengthen the climatological residual circulation, although the structure of the anomalies is different than the climatology. For example, the induced upwelling is centered on the equator whereas the maximum climatological upwelling is centered in the summer hemisphere, and the induced upwelling is strongest above the level of maximum aerosol radiative heating, and even negative below. This latter point may explain why post-Pinatubo anomalies in tropical upwelling are not apparent in observational records, which are usually displayed as timeseries of upwelling in the lower stratosphere (Seviour et al., 2012). We have shown that increased wave activity and wave drag in both hemispheres is a robust model response to volcanic aerosol forcing, and therefore a component of the residual circulation anomalies in the volcanically-forced

The impact of volcanic aerosol on the NH stratospheric polar vortex

M. Toohey et al.

Title Page

Abstract

Introduction

Conclusions

References

Tables

Figures



Back

Close

Full Screen / Esc

Printer-friendly Version

Interactive Discussion



The impact of volcanic aerosol on the NH stratospheric polar vortex

M. Toohey et al.

Title Page

Abstract

Introduction

Conclusions

References

Tables

Figures



Back

Close

Full Screen / Esc

Printer-friendly Version

Interactive Discussion



historical experiments (Charlton-Perez et al., 2013; Driscoll et al., 2012). We have shown that the meridional temperature gradient in the extratropical lower stratosphere induced by volcanic aerosol forcing, and therefore the strength of the induced stratospheric winter polar vortex wind anomalies, is controlled primarily by dynamical heating associated with the induced residual circulation rather than the direct aerosol radiative heating. The vortex response in the model is therefore much less robust than would be expected if it were directly due to the aerosol radiative heating, as it is instead subject to complexity and variability of wave-mean flow interaction in the winter stratosphere.

Our results further imply that the NH polar vortex response is quite sensitive to the specific structure of the volcanic forcing used. While all forcing sets lead to an overall increase in resolved wave activity in the stratosphere, the meridional structure of wave activity and wave drag anomalies, and hence the structure of the induced residual circulation, is seen to depend on the forcing set used. Compared to the S98 and SVC forcing sets, SAGE_4 λ and WVC produced stronger high latitude wave drag and residual circulation cell anomalies which extended farther into the polar latitudes, and correspondingly weaker polar vortices. We speculate that such sensitivity is due to the role that minor differences in volcanically induced temperature and wind anomalies play in wave-mean flow interactions in the stratosphere. This implies that – at least for a Pinatubo magnitude eruption – very accurate reconstructions of volcanic aerosol forcing would be required to reproduce any impact of the aerosols on polar vortex strength in climate model simulations.

Acknowledgements. The authors would like to thank C. Li for providing model restart fields for half of the MPI-ESM ensemble members. This work was supported by the Federal Ministry for Education and Research in Germany (BMBF) through the research program “MiKlip” (FKZ:01LP130B(MT):/01LP1130A(CT,MB)).

Computations were done at the German Climate Computer Center (DKRZ). We acknowledge the European Centre for Medium-range Weather Forecasts (ECMWF) for our use of ERA-Interim reanalysis data.

The service charges for this open access publication
16800

have been covered by a Research Centre of the Helmholtz Association.

References

- Andrews, D. G., Holton, J. R., and Leovy, C. B.: Middle Atmosphere Dynamics, Academic Press, New York, USA, 1987.
- Aquila, V., Oman, L. D., Stolarski, R., Douglass, A. R., and Newman, P. A.: The response of ozone and nitrogen dioxide to the eruption of Mt. Pinatubo at southern and northern midlatitudes, *J. Atmos. Sci.*, 70, 894–900, doi:10.1175/JAS-D-12-0143.1, 2013.
- Arfeuille, F., Luo, B. P., Heckendorn, P., Weisenstein, D., Sheng, J. X., Rozanov, E., Schraner, M., Brönnimann, S., Thomason, L. W., and Peter, T.: Modeling the stratospheric warming following the Mt. Pinatubo eruption: uncertainties in aerosol extinctions, *Atmos. Chem. Phys.*, 13, 11221–11234, doi:10.5194/acp-13-11221-2013, 2013.
- Baldwin, M. P. and Dunkerton, T. J.: Stratospheric harbingers of anomalous weather regimes, *Science*, 294, 581–584, doi:10.1126/science.1063315, 2001.
- Bittner, M., Timmreck, C., Schmidt, H., Toohey, M., and Krüger, K.: Sensitivity of the Northern Hemisphere winter stratosphere variability to the strength of volcanic eruptions, in preparation, 2014.
- Charlton-Perez, A. J., Baldwin, M. P., Birner, T., Black, R. X., Butler, A. H., Calvo, N., Davis, N. A., Gerber, E. P., Gillett, N., Hardiman, S., Kim, J., Krüger, K., Lee, Y.-Y., Manzini, E., McDaniel, B. A., Polvani, L., Reichler, T., Shaw, T. A., Sigmund, M., Son, S.-W., Toohey, M., Wilcox, L., Yoden, S., Christiansen, B., Lott, F., Shindell, D., Yukimoto, S., and Watanabe, S.: On the lack of stratospheric dynamical variability in low-top versions of the CMIP5 models, *J. Geophys. Res.-Atmos.*, 118, 2494–2505, doi:10.1002/jgrd.50125, 2013.
- Chen, P. and Robinson, W. A.: Propagation of planetary waves between the troposphere and stratosphere, *J. Atmos. Sci.*, 49, 2533–2545, doi:10.1175/1520-0469(1992)049<2533:POPWBT>2.0.CO;2, 1992.
- Christiansen, B.: Volcanic eruptions, large-scale modes in the Northern Hemisphere, and the El Niño–Southern Oscillation, *J. Climate*, 21, 910, doi:10.1175/2007JCLI1657.1, 2008.
- Crowley, T., Zielinski, G., Vinther, B. M., Udisti, R., Kreutz, K., Cole-Dai, J., and Castellano, E.: Volcanism and the little ice age, *PAGES news*, 16, 22–23, 2008.

The impact of volcanic aerosol on the NH stratospheric polar vortex

M. Toohey et al.

Title Page

Abstract

Introduction

Conclusions

References

Tables

Figures



Back

Close

Full Screen / Esc

Printer-friendly Version

Interactive Discussion



The impact of volcanic aerosol on the NH stratospheric polar vortex

M. Toohey et al.

Title Page

Abstract

Introduction

Conclusions

References

Tables

Figures



Back

Close

Full Screen / Esc

Printer-friendly Version

Interactive Discussion



Dee, D. P., Uppala, S. M., Simmons, A. J., Berrisford, P., Poli, P., Kobayashi, S., Andrae, U.,
Balmaseda, M. A., Balsamo, G., Bauer, P., Bechtold, P., Beljaars, A. C. M., van de Berg, L.,
Bidlot, J., Bormann, N., Delsol, C., Dragani, R., Fuentes, M., Geer, A. J., Haimberger, L.,
Healy, S. B., Hersbach, H., Hólm, E. V., Isaksen, I., Kållberg, P., Köhler, M., Matricardi, M.,
5 McNally, A. P., Monge-Sanz, B. M., Morcrette, J.-J., Park, B.-K., Peubey, C., de Rosnay, P.,
Tavolato, C., Thépaut, J.-N., and Vitart, F.: The ERA-Interim reanalysis: configuration and
performance of the data assimilation system, *Q. J. Roy. Meteor. Soc.*, 137, 553–597,
doi:10.1002/qj.828, 2011.

Driscoll, S., Bozzo, A., Gray, L. J., Robock, A., and Stenchikov, G.: Coupled Model Intercom-
parison Project 5 (CMIP5) simulations of climate following volcanic eruptions, *J. Geophys.*
10 *Res.*, 117, D17105, doi:10.1029/2012JD017607, 2012.

Eyring, V. and Lamarque, J.-F.: Overview of IGAC/SPARC Chemistry–Climate Model Initiative
(CCMI) community simulations in support of upcoming ozone and climate assessments,
SPARC Newsl., 40, 48–66, 2013.

15 Garcia, R. R. and Randel, W. J.: Acceleration of the Brewer–Dobson circulation due to in-
creases in greenhouse gases, *J. Atmos. Sci.*, 65, 2731–2739, doi:10.1175/2008JAS2712.1,
2008.

Gerber, E. P., Butler, A., Calvo, N., Charlton-Perez, A., Giorgetta, M., Manzini, E., Perlwitz, J.,
Polvani, L. M., Sassi, F., Scaife, A. A., Shaw, T. A., Son, S.-W., and Watanabe, S.: Assessing
20 and understanding the impact of stratospheric dynamics and variability on the Earth system,
B. Am. Meteorol. Soc., 93, 845–859, doi:10.1175/BAMS-D-11-00145.1, 2012.

Giorgetta, M. A., Jungclaus, J., Reick, C. H., Legutke, S., Bader, J., Böttinger, M., Brovkin, V.,
Crueger, T., Esch, M., Fieg, K., Glushak, K., Gayler, V., Haak, H., Hollweg, H.-D., Ilyina, T.,
Kinne, S., Kornblueh, L., Matei, D., Mauritsen, T., Mikolajewicz, U., Mueller, W., Notz, D., Pi-
25 than, F., Raddatz, T., Rast, S., Redler, R., Roeckner, E., Schmidt, H., Schnur, R., Segsnei-
der, J., Six, K. D., Stockhause, M., Timmreck, C., Wegner, J., Widmann, H., Wieners, K.-H.,
Claussen, M., Marotzke, J., and Stevens, B.: Climate and carbon cycle changes from 1850
to 2100 in MPI-ESM simulations for the coupled model intercomparison project phase 5, *J.*
Adv. Model. Earth Syst., 5, 572–597, doi:10.1002/jame.20038, 2013.

30 Graf, H.-F., Kirchner, I., Robock, A., and Schult, I.: Pinatubo eruption winter climate effects:
model versus observations, *Clim. Dynam.*, 9, 81–93, doi:10.1007/BF00210011, 1993.

Graf, H.-F., Li, Q., and Giorgetta, M. A.: Volcanic effects on climate: revisiting the mechanisms,
Atmos. Chem. Phys., 7, 4503–4511, doi:10.5194/acp-7-4503-2007, 2007.

The impact of volcanic aerosol on the NH stratospheric polar vortex

M. Toohey et al.

Title Page

Abstract

Introduction

Conclusions

References

Tables

Figures



Back

Close

Full Screen / Esc

Printer-friendly Version

Interactive Discussion



Kirchner, I., Stenchikov, G. L., Graf, H.-F., Robock, A., and Antuña, J. C.: Climate model simulation of winter warming and summer cooling following the 1991 Mount Pinatubo volcanic eruption, *J. Geophys. Res.*, 104, 19039–19055, doi:10.1029/1999JD900213, 1999.

Kodera, K.: Influence of volcanic eruptions on the troposphere through stratospheric dynamical processes in the Northern Hemisphere winter, *J. Geophys. Res.*, 99, D01273, doi:10.1029/93JD02731, 1994.

Kodera, K.: On the origin and nature of the interannual variability of the winter stratospheric circulation in the Northern Hemisphere, *J. Geophys. Res.*, 100, 14077, doi:10.1029/95JD01172, 1995.

Labitzke, K. and McCormick, M. P.: Stratospheric temperature increases due to Pinatubo aerosols, *Geophys. Res. Lett.*, 19, 207–210, doi:10.1029/91GL02940, 1992.

Labitzke, K. and van Loon, H.: The Southern Oscillation. Part IX: The influence of volcanic eruptions on the Southern Oscillation in the stratosphere, *J. Climate*, 2, 1223–1226, doi:10.1175/1520-0442(1989)002<1223:TSOPIT>2.0.CO;2, 1989.

Marshall, A. G., Scaife, A. A., and Ineson, S.: Enhanced seasonal prediction of European winter warming following volcanic eruptions, *J. Climate*, 22, 6168, doi:10.1175/2009JCLI3145.1, 2009.

McLandress, C. and Shepherd, T. G.: Simulated anthropogenic changes in the Brewer–Dobson circulation, including its extension to high latitudes, *J. Climate*, 22, 1516–1540, doi:10.1175/2008JCLI2679.1, 2009.

Muthers, S., Anet, J. G., Raible, C. C., Brönnimann, S., Rozanov, E., Arfeuille, F., Peter, T., Shapiro, A. I., Beer, J., Steinhilber, F., Brugnara, Y., and Schmutz, W.: Northern hemispheric winter warming pattern after tropical volcanic eruptions: sensitivity to the ozone climatology, *J. Geophys. Res.-Atmos.*, 119, 1340–1355, doi:10.1002/2013JD020138, 2014.

Newman, P. A. and Rosenfield, J. E.: Stratospheric thermal damping times, *Geophys. Res. Lett.*, 24, 433–436, doi:10.1029/96GL03720, 1997.

Newman, P. A., Nash, E. R., and Rosenfield, J. E.: What controls the temperature of the Arctic stratosphere during the spring?, *J. Geophys. Res.*, 106, 19999, doi:10.1029/2000JD000061, 2001.

Perlwitz, J. and Graf, H.-F.: The statistical connection between tropospheric and stratospheric circulation of the Northern Hemisphere in winter, *J. Climate*, 8, 2281–2295, doi:10.1175/1520-0442(1995)008<2281:TSCBTA>2.0.CO;2, 1995.

The impact of volcanic aerosol on the NH stratospheric polar vortex

M. Toohey et al.

Title Page

Abstract

Introduction

Conclusions

References

Tables

Figures



Back

Close

Full Screen / Esc

Printer-friendly Version

Interactive Discussion



Pitari, G.: A numerical study of the possible perturbation of stratospheric dynamics due to Pinatubo aerosols – implications for tracer transport, *J. Atmos. Sci.*, 50, 2443–2461, doi:10.1175/1520-0469(1993)050<2443:ANSOTP>2.0.CO;2, 1993.

Pitari, G. and Mancini, E.: Short-term climatic impact of the 1991 volcanic eruption of Mt. Pinatubo and effects on atmospheric tracers, *Nat. Hazards Earth Syst. Sci.*, 2, 91–108, doi:10.5194/nhess-2-91-2002, 2002.

Poberaj, C. S., Staehelin, J., and Brunner, D.: Missing stratospheric ozone decrease at Southern Hemisphere middle latitudes after Mt. Pinatubo: a dynamical perspective, *J. Atmos. Sci.*, 68, 1922–1945, doi:10.1175/JAS-D-10-05004.1, 2011.

Polvani, L. M. and Waugh, D. W.: Upward wave activity flux as a precursor to extreme stratospheric events and subsequent anomalous surface weather regimes, *J. Climate*, 17, 3548–3554, doi:10.1175/1520-0442(2004)017<3548:UWAFAA>2.0.CO;2, 2004.

Robock, A.: Volcanic eruptions and climate, *Rev. Geophys.*, 38, 191–219, doi:10.1029/1998RG000054, 2000.

Robock, A. and Mao, J.: Winter warming from large volcanic eruptions, *Geophys. Res. Lett.*, 19, 2405, doi:10.1029/92GL02627, 1992.

Rozanov, E. V.: Climate/chemistry effects of the Pinatubo volcanic eruption simulated by the UIUC stratosphere/troposphere GCM with interactive photochemistry, *J. Geophys. Res.*, 107, 4594, doi:10.1029/2001JD000974, 2002.

Russell, P. B., Livingston, J. M., Pueschel, R. F., Bauman, J. J., Pollack, J. B., Brooks, S. L., Hamill, P., Thomason, L. W., Stowe, L. L., Deshler, T., Dutton, E. G., and Bergstrom, R. W.: Global to microscale evolution of the Pinatubo volcanic aerosol derived from diverse measurements and analyses, *J. Geophys. Res.*, 101, 18745–18763, doi:10.1029/96JD01162, 1996.

Sato, M., Hansen, J. E., McCormick, M. P., and Pollack, J. B.: Stratospheric aerosol optical depths, 1850–1990, *J. Geophys. Res.*, 98, 22987–22994, doi:10.1029/93JD02553, 1993.

Schmidt, H., Rast, S., Bunzel, F., Esch, M., Giorgetta, M., Kinne, S., Krismer, T., Stenichkov, G., Timmreck, C., Tomassini, L., and Walz, M.: Response of the middle atmosphere to anthropogenic and natural forcings in the CMIP5 simulations with the Max Planck Institute Earth system model, *J. Adv. Model. Earth Syst.*, 5, 98–116, doi:10.1002/jame.20014, 2013.

Seviour, W. J. M., Butchart, N., and Hardiman, S. C.: The Brewer–Dobson circulation inferred from ERA-Interim, *Q. J. Roy. Meteor. Soc.*, 138, 878–888, doi:10.1002/qj.966, 2012.

The impact of volcanic aerosol on the NH stratospheric polar vortex

M. Toohey et al.

Title Page

Abstract

Introduction

Conclusions

References

Tables

Figures



Back

Close

Full Screen / Esc

Printer-friendly Version

Interactive Discussion



- Shepherd, T. G. and McLandress, C.: A robust mechanism for strengthening of the Brewer–Dobson circulation in response to climate change: critical-layer control of subtropical wave breaking, *J. Atmos. Sci.*, 68, 784–797, doi:10.1175/2010JAS3608.1, 2011.
- Shindell, D. T.: Dynamic winter climate response to large tropical volcanic eruptions since 1600, *J. Geophys. Res.*, 109, D05104, doi:10.1029/2003JD004151, 2004.
- Shindell, D. T., Schmidt, G. A., Miller, R. L., and Rind, D.: Northern Hemisphere winter climate response to greenhouse gas, ozone, solar, and volcanic forcing, *J. Geophys. Res.*, 106, D07193, doi:10.1029/2000JD900547, 2001.
- Stenchikov, G.: Arctic oscillation response to the 1991 Mount Pinatubo eruption: effects of volcanic aerosols and ozone depletion, *J. Geophys. Res.*, 107, 4803, doi:10.1029/2002JD002090, 2002.
- Stenchikov, G., Kirchner, I., Robock, A., Graf, H.-F., Antuña, J. C., Grainger, R. G., Lambert, A., and Thomason, L.: Radiative forcing from the 1991 Mount Pinatubo volcanic eruption, *J. Geophys. Res.*, 103, 13837–13857, doi:10.1029/98JD00693, 1998.
- Stenchikov, G., Hamilton, K., Stouffer, R. J., Robock, A., Ramaswamy, V., Santer, B., and Graf, H.-F.: Arctic Oscillation response to volcanic eruptions in the IPCC AR4 climate models, *J. Geophys. Res.*, 111, D07107, doi:10.1029/2005JD006286, 2006.
- Thomason, L. W. and Peter, T. (Eds.): Assessment of Stratospheric Aerosol Properties (ASAP), SPARC Report No. 4, WCRP-124, WMO/TD-No. 1295, 2006.
- Timmreck, C., Lorenz, S. J., Crowley, T. J., Kinne, S., Raddatz, T. J., Thomas, M. A., and Jungclaus, J. H.: Limited temperature response to the very large AD 1258 volcanic eruption, *Geophys. Res. Lett.*, 36, L21708, doi:10.1029/2009GL040083, 2009.
- Timmreck, C., Graf, H.-F., Lorenz, S. J., Niemeier, U., Zanchettin, D., Matei, D., Jungclaus, J. H., and Crowley, T. J.: Aerosol size confines climate response to volcanic super-eruptions, *Geophys. Res. Lett.*, 37, L24705, doi:10.1029/2010GL045464, 2010.
- Toohey, M., Krüger, K., Niemeier, U., and Timmreck, C.: The influence of eruption season on the global aerosol evolution and radiative impact of tropical volcanic eruptions, *Atmos. Chem. Phys.*, 11, 12351–12367, doi:10.5194/acp-11-12351-2011, 2011.

The impact of volcanic aerosol on the NH stratospheric polar vortex

M. Toohey et al.

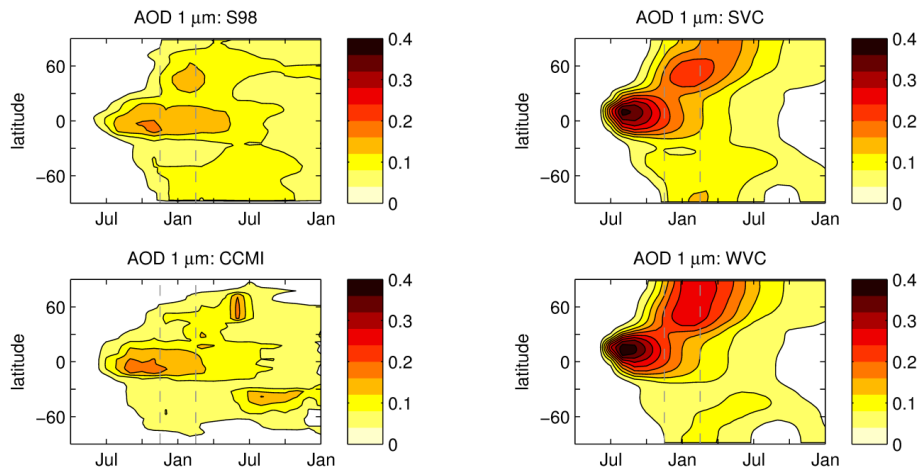


Figure 1. Zonal mean aerosol optical depth at 1 μm timeseries for the Pinatubo eruption, as reconstructed from observations producing the S98 and SAGE_4 λ forcing datasets (left) and based on MAECHAM5-HAM model simulations (right) and composited according to strong (SVC) and weak (WVC) vortex states. Gray vertical lines demarcate the DJF period of interest.

[Title Page](#)[Abstract](#)[Introduction](#)[Conclusions](#)[References](#)[Tables](#)[Figures](#)[◀](#)[▶](#)[◀](#)[▶](#)[Back](#)[Close](#)[Full Screen / Esc](#)[Printer-friendly Version](#)[Interactive Discussion](#)

The impact of volcanic aerosol on the NH stratospheric polar vortex

M. Toohey et al.

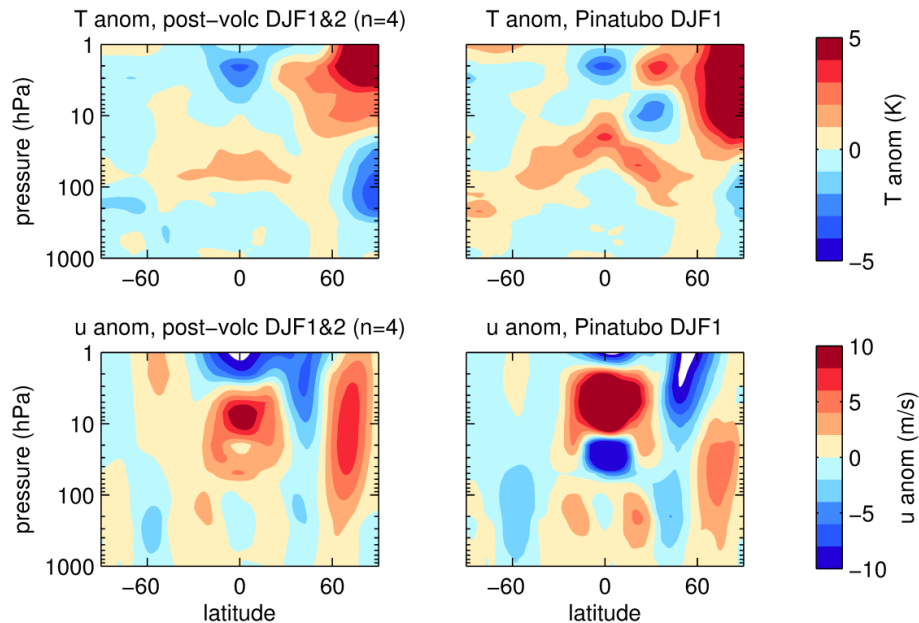


Figure 3. ERA-Interim DJF (top) temperature and (bottom) zonal wind anomalies for (left) post-volcanic composite ($n = 4$) of two winters after eruptions of El Chichón and Pinatubo, and (right) 1991/92, the first winter after the Pinatubo eruption.

[Title Page](#)
[Abstract](#)
[Introduction](#)
[Conclusions](#)
[References](#)
[Tables](#)
[Figures](#)
[Back](#)
[Close](#)
[Full Screen / Esc](#)
[Printer-friendly Version](#)
[Interactive Discussion](#)


The impact of volcanic aerosol on the NH stratospheric polar vortex

M. Toohey et al.

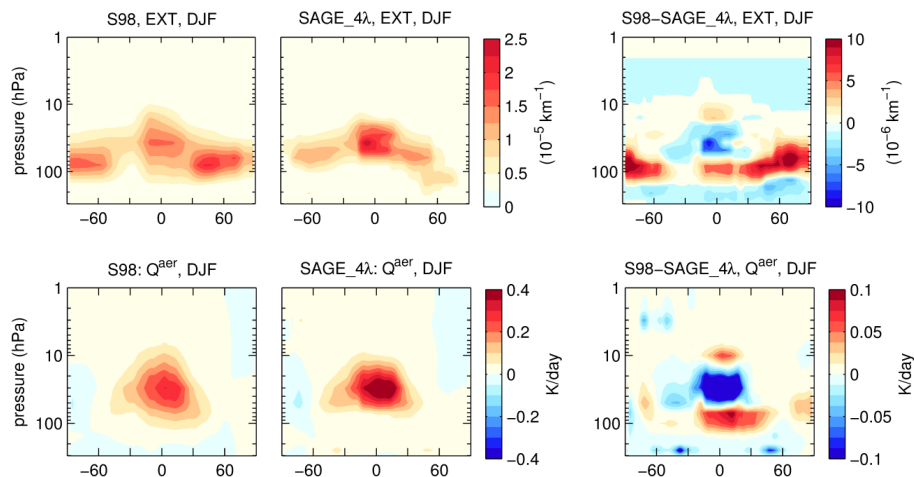


Figure 4. (Top) latitude-pressure distributions of $1\ \mu\text{m}$ aerosol extinction in the S98 and SAGE_4 λ volcanic aerosol forcing sets in first DJF after Pinatubo (winter 1991/92). (Bottom) aerosol radiative heating (Q^{aer}) as computed within the MPI-ESM model for each forcing set. Right-hand column shows S98-SAGE_4 λ differences for both $1\ \mu\text{m}$ extinction and Q^{aer} .

Title Page

Abstract

Introduction

Conclusions

References

Tables

Figures



Back

Close

Full Screen / Esc

Printer-friendly Version

Interactive Discussion



The impact of volcanic aerosol on the NH stratospheric polar vortex

M. Toohey et al.

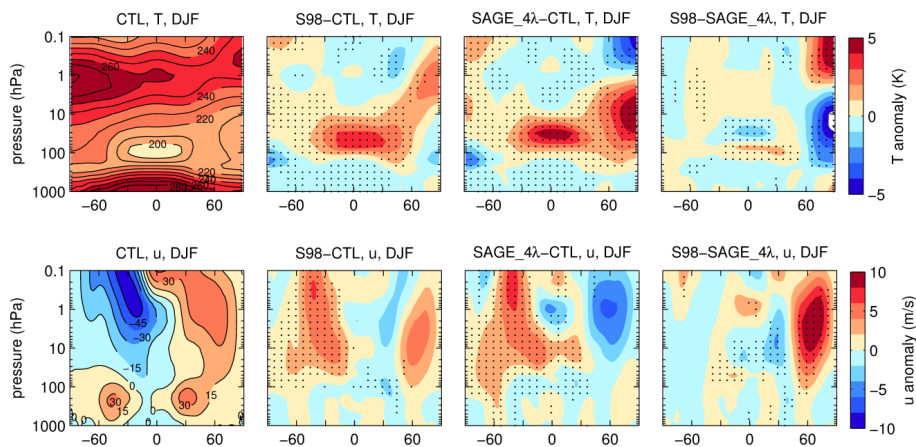


Figure 5. (Column 1) NH winter (DJF) control (top) temperature and (bottom) zonal wind; (columns 2 and 3) first post-eruption ensemble mean anomalies for S98 and SAGE_{4λ} forcing, and (column 4) difference between forced runs. Hatching highlights anomalies which are significant at the 95 % confidence level based on a bootstrapping algorithm.

Title Page

Abstract

Introduction

Conclusions

References

Tables

Figures

◀

▶

◀

▶

Back

Close

Full Screen / Esc

Printer-friendly Version

Interactive Discussion



The impact of volcanic aerosol on the NH stratospheric polar vortex

M. Toohey et al.

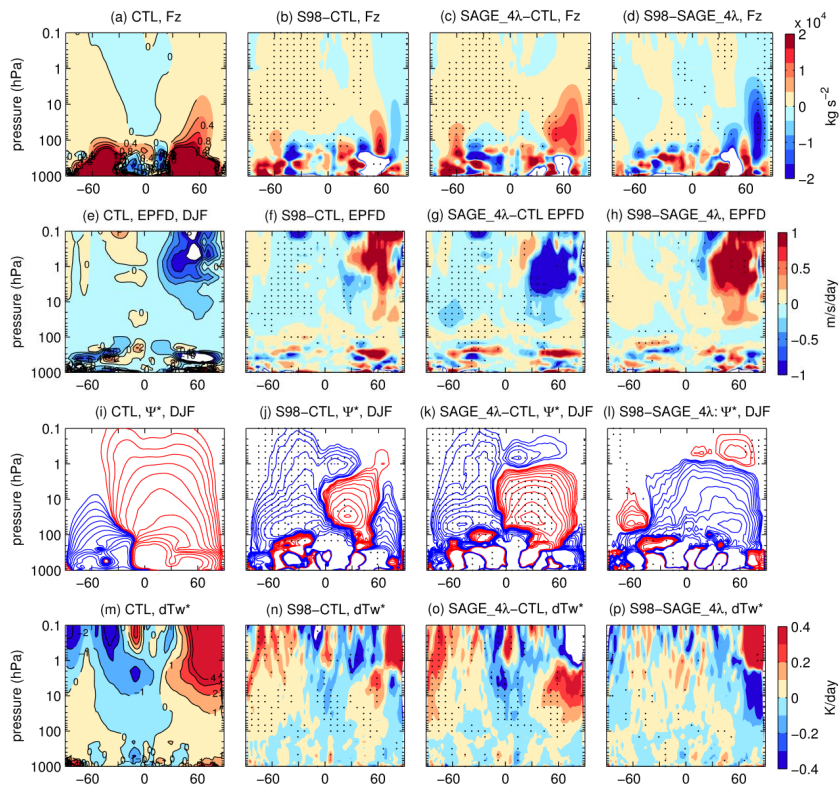


Figure 6. (Column 1) NH winter (DJF) control (rows, top-to-bottom) EP-flux vertical component, EP-flux divergence, residual stream function (red: clockwise; blue: counter-clockwise), and heating resulting from vertical advection; (columns 2 and 3) first post-eruption ensemble mean anomalies for S98 and SAGE_{4λ} forcing, and (column 4) difference between forced runs. Hatching highlights anomalies which are significant at the 95% confidence level based on a bootstrapping algorithm. Stream function contours in (i) are log-spaced, ranging from 10 to 10⁴ kg m⁻¹ s⁻¹, while those in (j, k, l) are log-spaced ranging from 1 to 100 kg m⁻¹ s⁻¹.

The impact of volcanic aerosol on the NH stratospheric polar vortex

M. Toohey et al.

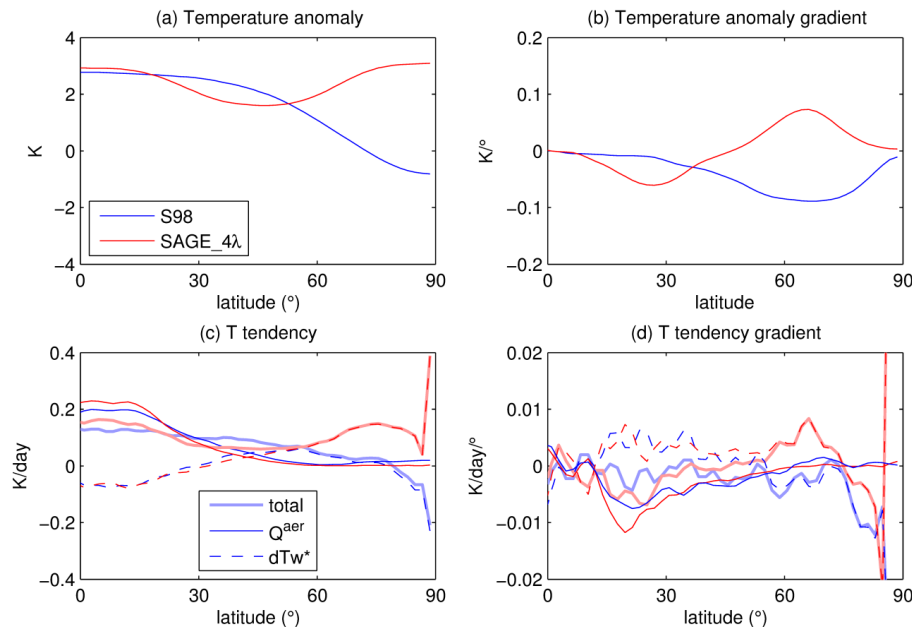


Figure 7. Lower stratospheric (100–20 hPa), DJF average thermodynamic quantities from the S98 and SAGE_4λ forced ensembles: **(a)** temperature anomalies, **(b)** meridional gradient of temperature anomalies, **(c)** temperature tendencies due to vertical advection (dashed thin), aerosol radiative heating (solid thin) and the sum of the two (solid thick lines), and **(d)** meridional gradients of the quantities in **(c)**.

[Title Page](#)
[Abstract](#)
[Introduction](#)
[Conclusions](#)
[References](#)
[Tables](#)
[Figures](#)
[Back](#)
[Close](#)
[Full Screen / Esc](#)
[Printer-friendly Version](#)
[Interactive Discussion](#)

The impact of volcanic aerosol on the NH stratospheric polar vortex

M. Toohey et al.

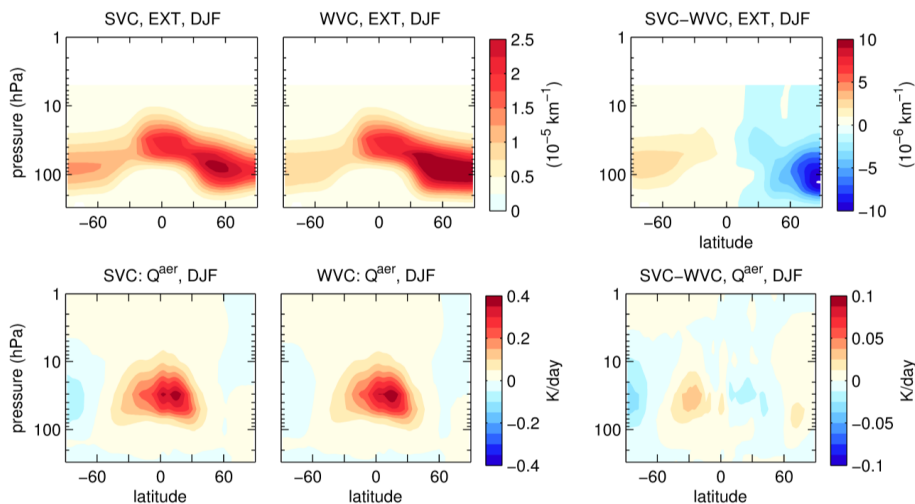


Figure 8. (Top) latitude-pressure distributions of $1\ \mu\text{m}$ aerosol extinction in the SVC and WVC volcanic aerosol forcing sets in first DJF after Pinatubo (winter 1991/92). (Bottom) aerosol radiative heating (Q^{aer}) as computed within the MPI-ESM model for each forcing set. Right-hand column shows SVC-WVC differences for both $1\ \mu\text{m}$ extinction and Q^{aer} .

Title Page

Abstract

Introduction

Conclusions

References

Tables

Figures

◀

▶

◀

▶

Back

Close

Full Screen / Esc

Printer-friendly Version

Interactive Discussion



The impact of volcanic aerosol on the NH stratospheric polar vortex

M. Toohey et al.

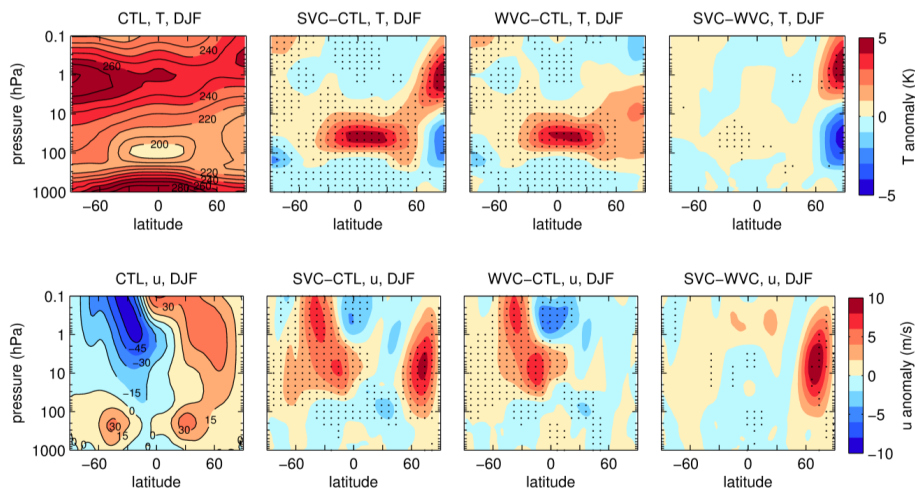


Figure 9. (Column 1) NH winter (DJF) control (top) temperature and (bottom) zonal wind; (columns 2 and 3) first post-eruption ensemble mean anomalies for SVC and WVC forcing, and (column 4) difference between forced runs. Hatching highlights anomalies which are significant at the 95% confidence level based on a bootstrapping algorithm.

Title Page

Abstract

Introduction

Conclusions

References

Tables

Figures

◀

▶

◀

▶

Back

Close

Full Screen / Esc

Printer-friendly Version

Interactive Discussion



The impact of volcanic aerosol on the NH stratospheric polar vortex

M. Toohey et al.

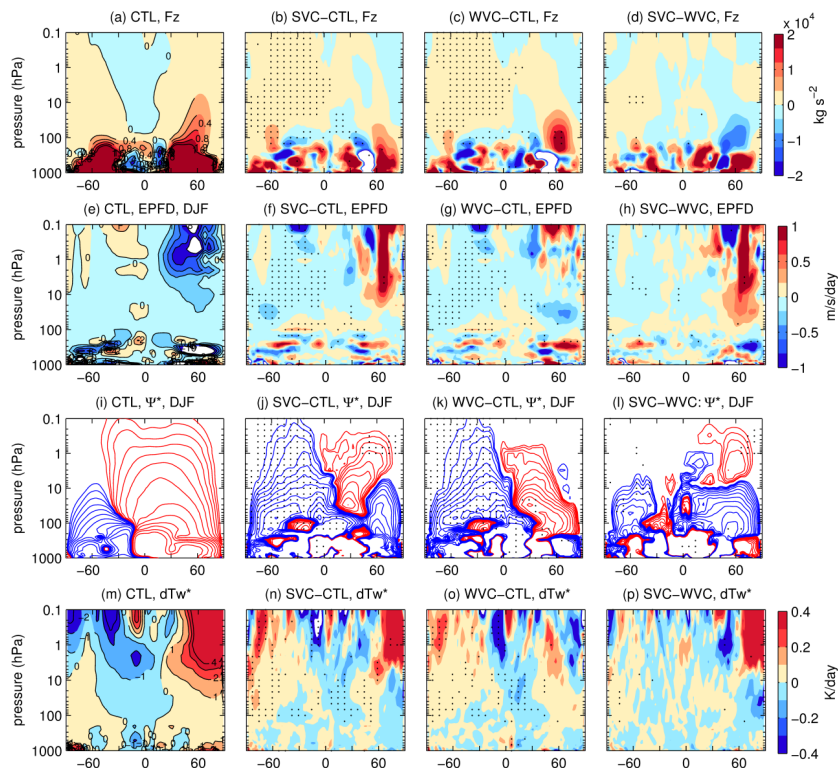


Figure 10. (Column 1) NH winter (DJF) control (rows, top-to-bottom) EP-flux vertical component, EP-flux divergence, residual stream function, and heating resulting from vertical advection; (columns 2 and 3) first post-eruption ensemble mean anomalies for SVC and WVC forcing, and (column 4) difference between forced runs. Hatching highlights anomalies which are significant at the 95 % confidence level based on a bootstrapping algorithm. Stream function contours in (i) are log-spaced, ranging from 10 to 10^4 $\text{kg m}^{-1} \text{s}^{-1}$, while those in (j, k, l) are log-spaced ranging from 1 to 100 $\text{kg m}^{-1} \text{s}^{-1}$.

The impact of volcanic aerosol on the NH stratospheric polar vortex

M. Toohey et al.

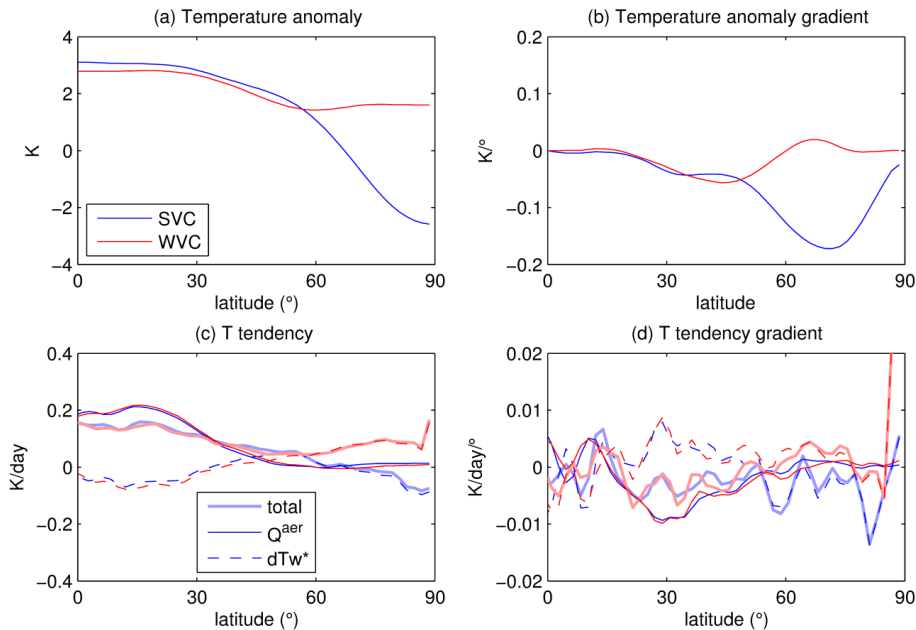


Figure 11. Lower stratospheric (100–20 hPa), DJF average thermodynamic quantities from the SVC and WVC forced ensembles: **(a)** temperature anomalies, **(b)** meridional gradient of temperature anomalies, **(c)** heating rates due to vertical advection (dashed thin), aerosol radiative heating (solid thin) and the sum of the two (solid thick lines), and **(d)** meridional gradients of the quantities in **(c)**.

The impact of volcanic aerosol on the NH stratospheric polar vortex

M. Toohey et al.

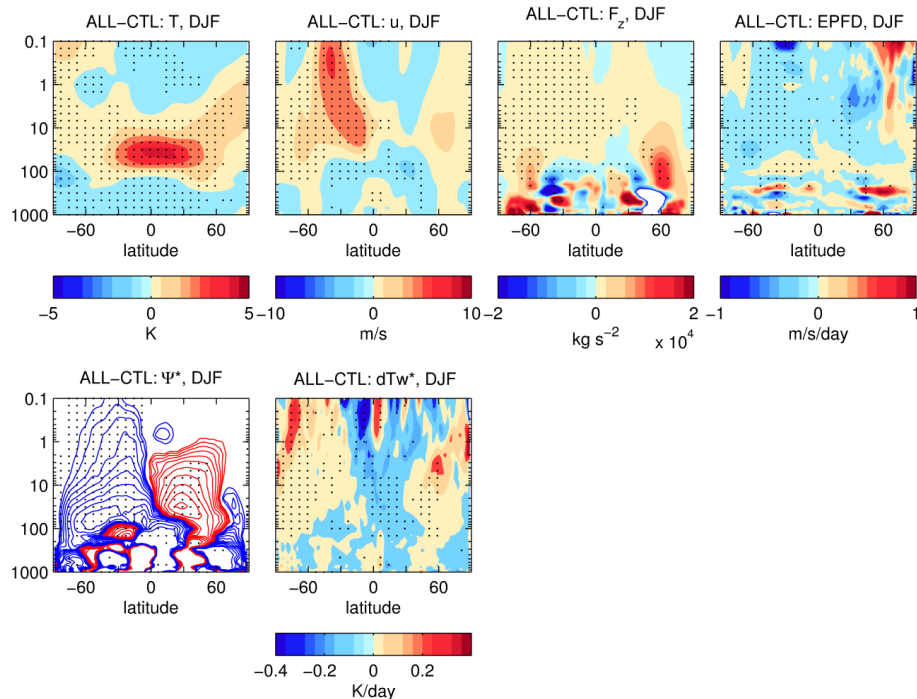


Figure 12. DJF anomalies for the ALL ensemble, i.e., the composite of all 4 forced ensembles. Shown are (a) temperature, (b) zonal wind, (c) vertical component of EP-flux, (d) EP-flux divergence, (e) residual circulation and (f) heating due to residual vertical advection. Streamfunction anomaly contours are as in Figs. 5 and 9.

The impact of volcanic aerosol on the NH stratospheric polar vortex

M. Toohey et al.

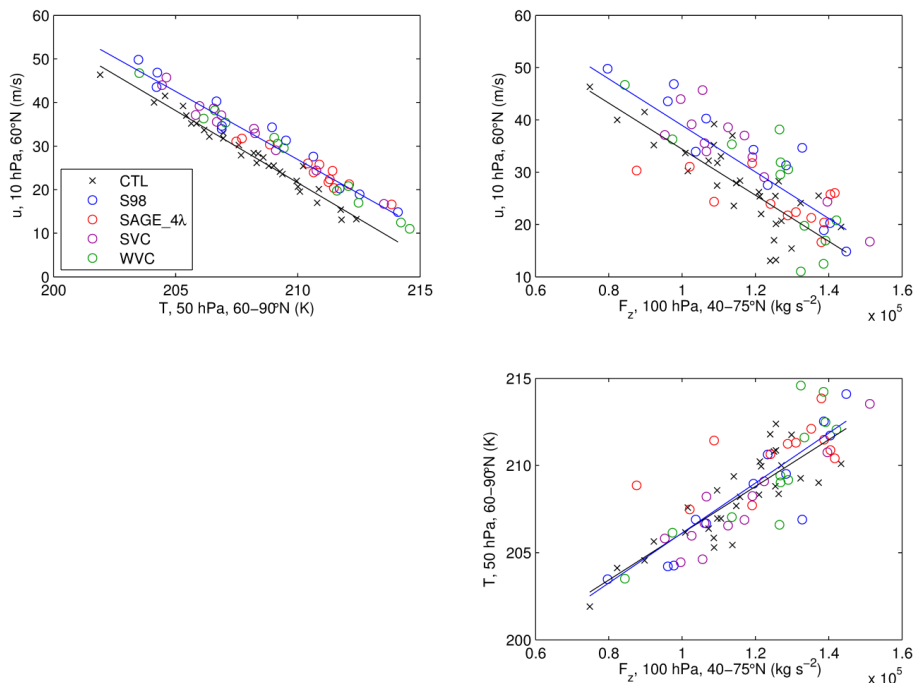


Figure 13. Scatter plots of selected quantities for the CTL and four volcanically forced ensembles. Shown are (upper left) zonal wind at 10 hPa, 60° N plotted against temperature at 50 hPa, 60–90° N averaged, (upper right) zonal wind at 10 hPa, 60° N plotted against the vertical component of EP-flux averaged over 40–75° N, and (lower right) temperature at 50 hPa, 60–90° N, plotted against the vertical component of EP-flux averaged over 40–75° N.

[Title Page](#)
[Abstract](#)
[Introduction](#)
[Conclusions](#)
[References](#)
[Tables](#)
[Figures](#)
[Back](#)
[Close](#)
[Full Screen / Esc](#)
[Printer-friendly Version](#)
[Interactive Discussion](#)


The impact of volcanic aerosol on the NH stratospheric polar vortex

M. Toohey et al.

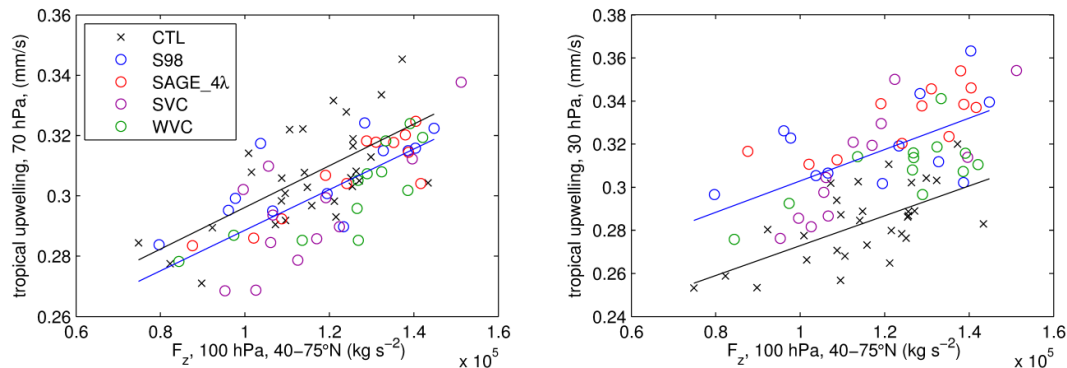


Figure 14. Scatter plots of tropical upwelling at 70 (left) and 30 hPa (right) vs. the vertical component of EP-flux at 100 hPa, averaged over 40–75° N, for the CTL and four volcanically forced ensembles.

Title Page

Abstract

Introduction

Conclusions

References

Tables

Figures

◀

▶

◀

▶

Back

Close

Full Screen / Esc

Printer-friendly Version

Interactive Discussion

